DOE-USD-SC0004768-FinalReport-01
DOE Award Number: DE-SC0004768

The University of South Dakota
414 East Clark Street, Vermillion, SD 57069

Crystal Growth and Detector Development for Underground Experiments

Principal Investor: Dongming Mei
August 06, 2018
Report Period: 05/16/2010 to 05/15/2018
Approved total budget: $3,424,378

1. Project Goal and Objectives

The goal of this project is to conduct material purification and crystal growth for ultra-low background experiments taking place at the Sanford Underground Research Facility (SURF, previously called DUSEL) in Lead, South Dakota. The objectives of the proposal are to reduce impurity levels of the grown crystals from ~10^{14}/cm^3 (commercially available) to ~10^{10}/cm^3 (detector-grade) and to increase the diameter of the grown crystals from 7 cm (commercially available) to 10 cm (underground experiments). Escalating the progress made in the past, we will improve technology with the following activities: 1) improving zone-refining methods in order to obtain an impurity level of ~1×10^{10}/cm^3, 2) implementing Monte Carlo simulations for crystal growth, 3) growing large detector-grade crystals for the ton scale Majorana and large scale SuperCDMS experiments, 4) automating the growth process, 5) comprehensively characterizing all grown crystals, 6) fabricating detectors with the grown crystals, and 7) developing new-type detectors to meet the needs of next generation experiments.

2. Description of accomplishments:

Fig. 1: Production of the zone-refined ingots per run with two stages and a total of 14 passes. Two ingots below the ruler are from the first stage and two ingots above the ruler are from the second stage. The net impurity levels are 6.0×10^{10}/cm^3, 7.7×10^{10}/cm^3, and 9.1×10^{10}/cm^3, for S1, S2, and S3, respectively.

The major foci of the project in the entire grant period were to continue developing methods to: (1) stabilize the zone refining parameters to consistently achieve an impurity level of ~10^{10}/cm^3 for the germanium ingots by optimizing a set of parameters for the zone speed, zone width, H_2 flow rate and pressure to produce 5.6 kg qualified ingots per run for multiple runs; (2) optimize crystal growth parameters to continue improving techniques for growing germanium crystals to achieve a large fraction (>30%) of detector-grade crystal by reducing residual impurities from the surrounding materials; (3) develop a characterization method for understanding mobility for high resistivity ingots or crystals through post-annealing process using a furnace filled with argon gas; and (4) fabricate the grown crystals into large-size detectors for studying the correlation between charge trapping and impurity level as well as mobility.

In the entire grant period, 05/16/2010 to 05/15/2018, we continue making significant progress toward our goal of producing high purity germanium crystals. Several milestones have been achieved as described below:

1) Zone refinement

Zone refined ingots with an impurity level of $\sim 10^{10}/cm^3$ is needed to grow detector-grade single crystals. We have achieved this level of impurity since the last grant period. However, as the input material to crystal growth, we need the production of qualified zone-refined ingots at least 3 kg per week. This requires the zone refining work to stabilize the run condition and continuously run for long period (about 10 days) to produce 5.6 kg qualified ingots. In a month, we need to demonstrate a production of 16.8 kg to meet the crystal growth needs. This production rate would allow us to grow crystals on weekly basis with the starting materials ranges from 3 kg to 6 kg. This production rate is determined based on a production of detector-grade crystals of 60 kg per year to significantly contribute to a ton-scale neutrinoless double-beta decay experiment, such as LEGEND, a newly formed global collaboration with 202 collaborators from 22 institutions across 14 countries. Figure 1 shows that we have met this milestone for the production of qualified zone-refined ingots at level of 5.6 kg per run in 10 days.

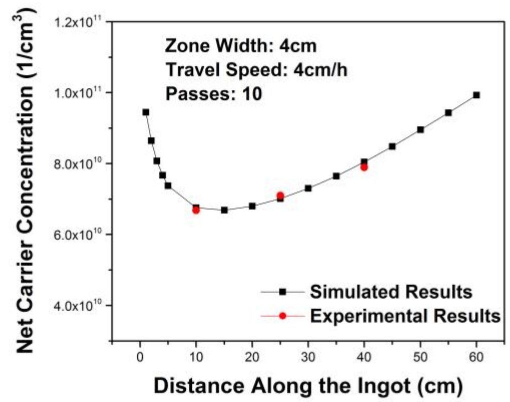

Fig. 2: The comparison between the prediction using Equation (1) and the experimental results.

The equation below predicts the net impurity level after ~14 passes to reduce B, Al, Ga, and P concentrations by 4 orders of magnitude assuming they exist monotonically in atomic format.

$$|N_A - N_D| = \sum_i^4 C_i(x)\left(1 - (1-k_i)e^{-\frac{k_i x}{L}}\right)^n \quad (1)$$

where $|N_A - N_D|$ is the remaining net impurity in the Ge ingot after zone refining, x is the length of the Ge ingots, $C_i(x)$ is the initial purity, i runs from 1 to 4 for B, Al, Ga, and P in the Ge ingot, respectively, k_i is the effective segregation coefficient in Ge, L is the width of the melting zone, n is the number of passes. A two-stage zone refining process has been adopted in our lab. We start with graphite boat to remove impurities from $\sim 10^{14}/cm^3$ to $\sim 10^{12}/cm^3$ and continue with a quartz boat to remove impurities from a level of $10^{12}/cm^3$ to $\sim 10^{10}/cm^3$. Three slices, S1, S2, and S3, were cut for Hall Effect measurements as shown in Figure 1.

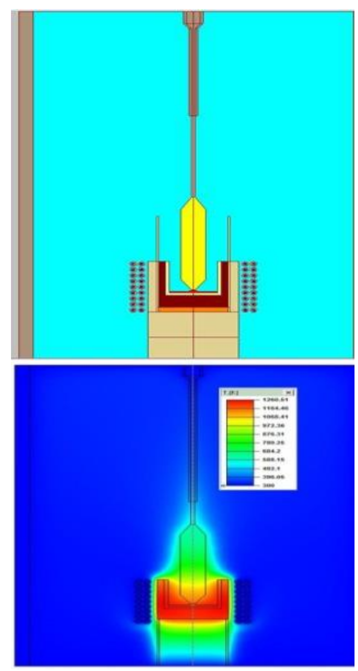

Fig. 3: Examples from the simulation of single crystal growth. **Top:** Geometry simulated in the software. **Bottom:** Heat transfer with a given power.

Figure 2 shows the comparison between the prediction using Equation (1) and the experimental data obtained recently (see caption of Figure 1). The impurity level in our zone-refined ingots has reached ~(6-9)×10^{10} per cm^3.

2) Crystal Growth

In the entire grant period, we have been focusing on improving successful rate of detector-grade crystals per growth. Since we grow crystals at least once per week, we intended to demonstrate a successful rate of 50% per growth. This means that we should have a portion of crystal to be detector-grade every two growths. This milestone was achieved in the beginning of 2017. Then, we wanted to demonstrate the fraction of detector-grade in a grown crystal is 30%. However, we have found that the fraction of the detector-grade crystals varies from 10% to 50%. This large variability indicates that we need to control the thermal field better. The thermal field is directly related to the growth rate. Ideally, a small growth rate is preferred. But one cannot grow too slow because the diameter of crystal would be too large. The growth rate and quality of HPGe crystals largely depend on the control of the thermal field (heat transfer and temperature profile). However, these control parameters can only be regulated externally. More specifically, they can only be regulated through growth system geometry, gas flow rate and pressure, pulling rate, frequency, and the power of the RF heater. Measurements inside the growth chamber (temperature over 1000^{o}C), and a quantitative determination of the control parameters are extremely challenging. Therefore, simulation and modeling of crystal growth play a vital role in developing innovative pulling procedures and augmenting crystal quality. Using FEMAG Soft, we have simulated single crystal growth to obtain information about radial/axial temperature gradient, radial heat flux, and axial heat flux for the furnace geometry with ambient H_2 gas. The simulation of the thermal field is shown in *Figure 3*.

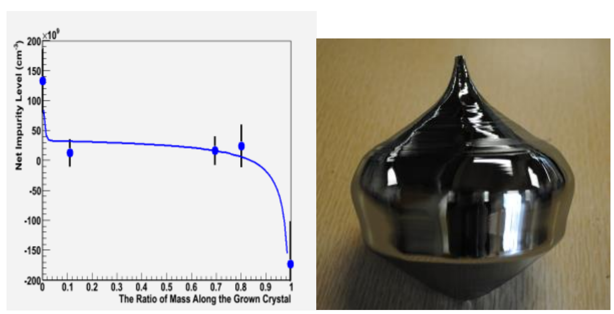

Fig. 4: A grown crystal with impurity level of 1-3 x10^{10}/cm^3 for large fraction of the crystal (~50%). Left: Experiment data point fitted with Equation (2). Right: the grown crystal in which the data points were obtained.

Large single crystals of Ge are grown using the Czochralski technique. We have published three papers on how to improve the quality of large-size crystals, demonstrating our ability to control the parameters for growth of low-dislocation (3,000 – 7,000 etch pits/cm^2), large diameter (~12 cm), and high-purity Ge single crystals (~10^{10}/cm^2) to be used for detector fabrication. With the implementation of the crystal growth simulation that takes into account furnace geometry, materials and operating conditions, and experimental results, higher mobility (>45,000 cm^2/Vs) crystals with uniform distribution of a level of impurity between 1 – 3 ×10^{10}/cm^3 and a diameter up to 12 cm was achieved within Year 7 and the fraction of detector-grade varies from 10% to 50%. Our goal in this grant period is to reduce the variability to 30% to 50%. We illustrate the strategy below. The net impurity can be calculated as

$$\left| N_A - N_D \right| = \sum_{i}^{4} C_i \times k_i \times (1-g)^{(k_i -} \quad (2)$$

with $|N_A-N_D|$ being the next impurity level after the growth, C_i the initial impurity of B, Al, Ga, and P, before the growth, i representing B, Al, Ga, and P, k_i the effective segregation coefficient for B, Al, Ga, and P, respectively, g is the fraction of crystal.

Utilizing the zone-refined ingot with an impurity level shown in Figure 2 as the input materials, the net impurity level can be calculated using Equation (2). A comparison between the Hall Effect measurements (data points) and the fitted function (solid line), Equation (2), is shown in Figure 4, where a high quality crystal with diameter up to 10 cm was achieved. The measured mobility is greater than 45,000 cm^2/Vs along both radial and axial axis. However, growing similar quality crystals with diameter up to 12 cm will require a much better control of the thermal gradient and impurity distribution in the radial direction during the crystal growth, which is usually difficult to achieve. The hypothesis is that the dislocations and impurities are outward distributions along the radial direction. Therefore, the zone-refined ingots with impurity level of $(1\text{-}3)\times10^{10}/cm^3$ must be used as the starting materials for crystal growth. A new thermal shield, which guarantees a small gradient in the radial direction, must be adopted to achieve our goal. Similarly to the last report period, we have been implementing the described methods to continue growing crystals for achieving larger portions to be detector-grade crystals. The biggest detector-grade crystals we have obtained are 2200 grams with diameter of ~10 cm.

3) Crystal Characterization

The characterization of a grown crystal provides necessary feedback to make improvements in the growth procedure. In addition to continuing Hall Effect measurements for understanding electrical properties, optical measurements for understanding dislocation density and a Photo thermal Ionization Spectroscopy (PTIS) to measure the shallow impurities in the grown crystals, we investigated mobility in high resistivity samples. In general, Hall voltage will not reverse in those high resistivity samples and mobility is very low at a level of a few thousands. Pioneers such as Dr. Gene Haller attributed this to p-n junction formed inside the sample, which requires additional treatment, for example, post-annealing to allow impurity to redistribute so that the p-n junctions disappear. After the annealing, the samples all show good Hall Effects. This post-annealing method allows us to study mobility as a function of ionized impurity, neutral impurity, and lattice scattering to find out which one is dominated at 77 K. This is important since constant charge draft mobility is used to simulate the pulse shape for separating multi-site events from single-site events in the germanium-based neutrinoless double-beta decay experiments such as GERDA and Majorana.

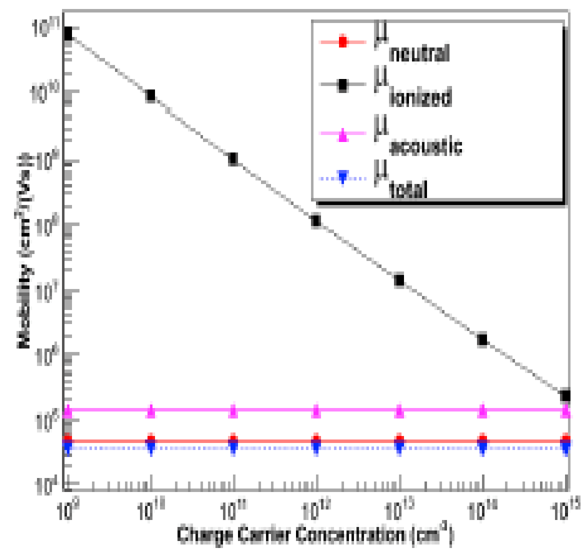

.
Fig.5: Mobility versus carrier concentration for all scattering mechanisms.

This is only true if the draft mobility is dominated by lattice scattering. However, what we found in our measurements is that both lattice scattering and neutral impurities are important when the ionized impurities at a level of $10^{10}/cm^3$ at which the contribution to the draft mobility is small as shown in Figure 5. Figure 5 shows the measured Hall mobility as a function of the ionized impurity. If both lattice scattering and neutral impurity contribute to the draft mobility at the same level, then the draft mobility cannot be a constant because the neutral impurity cannot be a constant for a given crystal. Thereofre, the pulse shape simulation must take into account the neutral impurity.

4) Detector development

The ultimate test of the quality of a high-purity crystal is to produce a detector from the material and evaluate it for electrical and spectral performance. We have fabricated 4 planar detectors with our collaborator at LBNL, Mark Amman (before he retired) in the grant period of 2015. The detectors worked as normal radiation detectors. In this grant period, we have fabricated detectors that have performance as shown in Figure 6. To convert a sample into a detector for such a performance, the following procedure was used. The sample was first cut to a cylinder. Following the cutting, the sample was lapped and then chemically polished in a 4:1 nitric to hydrofluoric acid mixture. After the mechanical and chemical processing, electrical contacts were formed on the sample. Amorphous semiconductor based electrical contacts were RF sputter deposited with the resultant structure. The first of two sputter depositions consisted of coating the top contact face and the sides of the crystal with amorphous Ge (a-Ge). The second deposition coated the bottom with amorphous Si (a-Si). Both depositions used an $Ar\text{-}H_2$ (7% H_2) gas mixture for the sputter gas. With the sample completely coated with amorphous semiconductor, Al was thermally evaporated onto both the top and bottom surfaces in order to complete the detector fabrication. In January of 2017, Mark Amman fabricated a larger crystal (8 cm in diameter and 1.5 cm in length) from USD crystal at LBNL. In the early of 2018, USD started fabricating small planar detectors using the home-grown crystals at USD. So far, nine small detectors were fabricated at USD with a successful rate of 66%. The failed ones are mainly two-wing detectors.

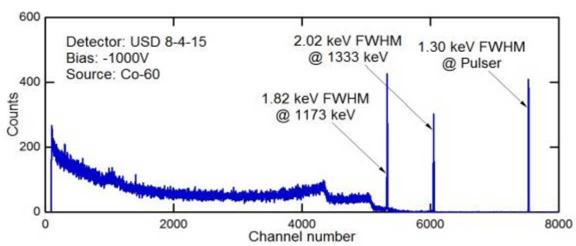

Fig. 6: A Co-60 spectrum measured using the fabricated detector with amorphous germanium contacts.

3. A list of papers and talks

In the entire report period, more than 20 papers were presented at the APS March meetings.

(1) A24.00004 XRD analysis of high purity germanium single crystals grown by Czochralski method, Gang Yang.
(2) A24.00013 Optimization of high purity germanium (HPGe) crystals growth rate through the simulation and modeling of growth system geometry. Jay Govani.
(3) A24.00010 Performance optimization of diffused Li on Ga/In eutectic, In/Sn solder and eutectic Ga/In Ohmic contacts to n-high purity-crystalline (100) Ge. Muhammad Khizar.
(4) A24.00009 Impact of atmosphere on HPGe crystal growth, Guojian Wang.

(5) A24.00011 Crystal-growth Underground Breeding Extra-sensitive Detectors, Dongming Mei.
(6) P33.00005 Si-SiGe hetero-structure thin-film solar cells using integrated electro-optical modeling, Muhammad Khizar.
(7) S24.00011 PTIS (Photo-Thermal Ionization Spectroscopy) and its application in HPGe purification and crystal growth. Yutong Guan
(8) Q44.00006 Investigation of influential parameters for zone-refinement of germanium crystals . Gang Yang.
(9) Q44.00005 The origin and distribution of phosphorus in large size HP-Ge crystals. Guojian Wang.
(10) Q44.00007 Dislocation distribution in large high-purity germanium crystal. Hao Mei.
(11) Q44.00008 Characterization of three planar germanium detectors fabricated with the crystals grown at USD. Jay Govani.
(12) M9.00006 Purification of Germanium Crystals by Zone Refinement: Theoretical and Experimental Approaches. Gang Yang.
(13) M9.00003 Crystal growth and detector performance of large size high-purity Ge crystals. Guojian Wang.
(14) M9.00004 Characterization of dislocation and defects for large high purity Ge crystals. Hao Mei.
(15) B51.00001 The impact of neutral impurity concentration on charge drift mobility, Hao Mei.
(16) B51.00002 Influences of solid/liquid boundary layer thickness and tilting angle on zone-refinement of germanium crystals, Gang Yang.
(17) B51.00011 Impact of Crystalline Structure on the Temperature Dependence of Resistivity, Yutong Guan.
(18) V7.00009 Impurity distribution in high purity germanium crystal and its impact on the detector performance. Guojian Wang.
(19) G1.00286 Electrical behaviors of high purity germanium at low temperature, Gnag Yang.
(20) P27.00007 The impact of neutral impurity concentration on charge drift mobility in N-type Ge crystals, Hao Mei
(21) P27.00008 Electrical behaviors of high purity germanium crystals at low temperature, Gang Yang.
(22) R28.00002 High-Purity Germanium Crystal Growth and the Performance of a SuperCDMS Detector Fabricated from a USD Crystal. Guojian Wang.
(23) Zone Refining, Crystal Growth and Characterization of HP-Ge at USD, PIRE-GEMADARC Workshop , Xichang, China, 2018. Guojian Wang.
(24) Zone Refining, Crystal Growth and Characterization of HP-Ge at USD, PIRE-GEMADARC Workshop , Berkeley, California, 2017. Guojian Wang.
(25) Growth and Characterization of Large HPGe crystals, 2017 International Germanium Detector Technology Workshop, Berkeley, California, 2017. Guopjian Wang.
(26) Crystal Growth, characterization and detector performance of High-purity Germanium crystals, Conference on Science at the Sanford Underground Research Facility 2017, Rapid City, South Dakota, 2017. Guojian Wang.
(27) CUBED crystal growth, Workshop on Germanium-Based Detectors and Technologies-2014, Vermillion, South Dakota, 2014. Guojian Wang.

In addition, Dr. Mei gave more than 20 invited talks at various conferences and seminars, including two invited talks given for SuperCDMS collaboration in 2015, two talks given for the LEGEND collaboration meeting in Atlanta in October 2016 and a talk in Cosmic Frontier workshop held in Maryland in March 2017 as well as serval invited talks given to the international germanium workshop at UC Berkeley in 2010, International germanium-based technology workshop at USD in 2014, and the international germanium-based detector and technology workshop at Lawrence Berkeley National Laboratory in 2017.

Two talks were presented in COSSURF conference in Rapids City, South Dakota School Mines and technology, May 13-15, 2017.

<u>Thirty papers were published in several journals:</u>

1. Electrical conductivity of high-purity germanium crystals at low temperature, G. Yang, Kyler Kooi, Guojian Wang, Hao Mei, Yangyang Li, and Dongming Mei, Applied Physics A, 124 (2018)381.
2. Direct detection of MeV-scale dark matter utilizing germanium internal amplification for the charge created by the ionization of Impurities, D.-M. Mei et al., Eur. Phys. J. C (2018) 78:187.
3. The electrical properties and distribution of indium in germanium crystals, G.-J. Wang, H. Mei, X.-H. Meng, G. Yang, D.-M. Mei, accepted for publication in Materials Science in Semiconductor Processing, Vol.74, 2018, 342-346.
4. Average energy expended per e-h pair for germanium-based dark matter experiments, W.-Z. Wei and D.-M. Mei, Journal of Instrumentation12 (2017) P04022. arXiv:1602.08005.
5. A comprehensive study of low-energy response for xenon-based dark matter experiments, L. Wang and D.-M. Mei, Journal of Physics G: Nuclear and Particle Physics 44 (2017) 055001, arXiv: 1604.01083.
6. The impact of neutral impurity concentration on charge drift mobility in n-type germanium, H. Mei, G.-W. Wang, G. Yang, D.-M. Mei, Journal of Instrumentation 12 (2017) P07003, arXiv：1705.09562.
7. Observation of annual modulation induced by γ rays from (α,γ) reactions at the Soudan Underground Laboratory, A. Tiwari, C. Zhang, D.- M. Mei and P. Cushman, Physics Review C 96 (2017) 044609, arXiv:1706.00100.
8. Cosmogenic activation of germanium used for tonne-scale rare event search experiments, W.-Z. Wei, D.-M. Mei, C. Zhang, arXiv: 1706.05324 (accepted by Astroparticle Physics, 96 (2017) 24-31.
9. The Large Enriched Germanium Experiment for Neutrinoless Double Beta Decay (LEGEND). The LEGEND Collaboration, arXiv:1709.01980, 2017.
10. US Cosmic Visions: New Ideas in Dark Matter 2017: Community Report. arXiv:1707.04591, 2017.
11. Discrimination of nuclear and electronic recoil events using plasma effect in germanium detectors, W.-Z. Wei, J. Liu, and D.-M. Mei, arXiv:1605.05244. JINST 11 (2016) no.07, P-07008.
12. Cosmogenic activation of materials used in rare event search experiments, C. Zhang, D.-M. Mei, V. A. Kudryavtsev, S. Fiorucci, arXiv:1603.00098, AstroParticle Physics 84 (2016) 62-69.

13. Impact of nuclear impurity concentration on charge drift mobility in germanium, H. Mei, D.-M. Mei, G.-J. Wang, G. Yang, arXiv: 1607.03032. Submitted to Journal of Instrumentation for publication.
14. High-purity germanium crystal growth at the University of South Dakota, Guojian Wang, Hao Mei, Dongming Mei, Yutong Guan, and Gang Yang, IOP Science Journal of Physics: Conference Series, V606 (2015) 012012.
15. Study on the properties of high-purity germanium crystals, G. Yang, H. Mei, Y.-T. Guan, G.-J. Wang, D.-M. Mei, K. Irmscher, IOP Science Journal of Physics: Conference Series, V606 (2015) 012013.
16. Zone refinement of germanium crystals, G. Yang, Y.-T. Guan, F.-Y. Jian, M.-D. Wanger, H. Mei, G.-J. Wang, S.-M. Howard, D.-M. Mei, A. Nelson, J. Marshai, K. Fitzgerald, C. Tenzin and X. Ma, IOP Science Journal of Physics: Conference Series, V606 (2015) 012014.
17. Study well-shaped germanium detectors for low-background counting, W.-Z. Wei, D.-M. Mei, and C. Zhao, IOP Science Journal of Physics: Conference Series, V606 (2015) 012019.
18. Iris Abt, Bela Majorovits, Christina Keller, Dongming Mei, Guojian Wang, Wenzhao Wei, 2nd Workshop on Germanium Detectors and Technologies, Journal of Physics: Conference Series 2015, 606, 011001.
19. G. Wang, Y. Sun, G. Yang, W. Xiang, Y. Guan, D.-M. Mei, C. Keller and Y.-D. Chan, "Development of large size high-purity germanium crystal growth," Journal of Crystal Growth, 352 (1), 27-30 (2012).
20. G. Wang, Yutong Guan, Hao Mei, Dongming Mei, Gnag Yang, Jayesh Govani, Muhammad Khizar, "Dislocation density control in high-purity germanium crystal growth," Journal of Crystal Growth, 393 (2014) 54-58.
21. G. Yang, Jayesh Govani, Hao Mei, Yutong Guan, Guojian Wang, Mianliang Huang and Dongming Mei, "Investigation of influential factors on the purification of zone-refined germanium ingot," Crystal Research and Technology, V 49, (2014) 269-275.
22. G. Yang, G. Wang, W. Xiang, Y. Guan, Y. Sun, D.-M. Mei, B. Gray, Y.-D. Chan, "Radial and axial impurity distribution in high-purity germanium crystals," Journal of Crystal Growth,352 (1), 43-46 (2012).
23. G. Yang, D.-M. Mei, J. Govani, G. Wang, M. Khizar, "Effect of annealing on contact performance and electrical properties of p-type high purity germanium single crystal," Applied Physics A, DOI 10.1007/s00339-012-7518-x (2013).
24. G. Wang, Y. Sun, Y. Guan, D.-M. Mei, G. Yang, A. A. Chiller, B. Gray, "Optical Methods in Orientation of High-Purity Germanium Crystal," Journal of Crystallization Process and Technology, 3, 60-63 (2013).
25. Measuring Muon-Induced Neutrons with Large Liquid Scintillation Detector at Soudan Mine , C. Zhang, D.-M. Mei, arXiv: 1407.3246. Phys. Rev D 90 (2014) 122003.
26. Measuring Double-Electron Capture with Liquid Xenon Experiments, D.-M. Mei et al., Phys. Rev. C 89 (2014) 014608.
27. Ionization Efficiency Study for Low Energy Nuclear Recoils in Germanium, D. Barker, W.-Z. Wei, D.-M. Mei, and C. Zhang, Astropartcile Physics. 48 (2013) 8-15.
28. Measuring Fast Neutrons using Large Liquid Scintillation Detector for Ultra-Low Background Experiments, C. Zhang, D.-M. Mei, P. Davis, B. Woltman, F. Gray, Nucl. Instr. And Meth. A, 729 (2013) 138-146.

29. Germanium Detector Response to Nuclear Recoils in Search for Dark Matter, D. Barker, D.-M. Mei, arXiv: 1203.4620. Astropart. Phys. 38 (2012) 1-6.
30. Muon-Induced Background Study for an Argon-Based Long Baseline Neutrino Experiment, D. Barker, D.-M. Mei, Chao Zhang, arXiv: 1202.5000. Phys. Rev. D 86, 054001 (2012).

Patent:

Guojian Wang, Dongming Mei, Method of growing germanium crystals, USA Patent. Application Number: PCT/US2014043231.

4. A list of people

The list of people who are working on the project (F: Faculty; P: Postdoc; T: Technician; G: Graduate Students; U: Undergraduate Students; R: Research Scientist; FTE: Full Time Effort)

Name	F	P	T	G	U	R	FTE	DOE	CUBED
Dongming Mei	y						0.6	33%	67%
Yongchen Sun	y						0.5	33%	33%
Vince Guiseppe	y						0.15	17%	
Chaoyang Jiang	y						0.5	33%	
Christina Keller*	y						0.1		
Dan Tracy	y						0.3	33%	
Stanley Howard	y						0.5		67%
Rob McTaggart	y						0.3		33%
Haiping Hong						y	0.17		10%
Guojiang Wang		y					1.0	100%	
Gang Yang		y					1.0		100%
Wenchnag Xiang		y					1.0		100%
Chao Zhang*		y					0.25		
Oleg Perezovchikov							0.25		100%
Yutong Guan			y				1.0	100%	
Keenan Thomas				y			0.25	100%	
Xiaoyi Yang				y			0.5	100%	
D'Ann Barker				y			0.5	100%	
Wenzhao Wei				y			0.5	100%	
Chris Chiller				y			0.5	100%	
Angela Chiller				y			0.5		100%
Dana Byram				y			0.5		100%
Hao Mei					y		0.25	100%	
Austin Nelson				y			0.5		100%
Abdul Mohammed				y			0.25		50%
Mahadem Hossain				y			0.25		50%
Iseley Marshall					y		0.25	100%	
Alyssa Day					y		0.25	100%	
Nick Weinandt					y		0.5	100%	
Dusty Nowotny					y		0.25	100%	

Andrew Schmitz					y		0.25	100%	
Logan Brekke					y		0.25	100%	
Kate Schlotterback					y		0.25	100%	
Fanyi Jian					y		0.25	100%	
Andrea Gillespie					y		0.25	100%	
Jaret Heise*						y	0.1		
Vernon Mcbride						y	0.15		33%
Edward Lewis*						y	0.15		
Muhammad Khizar	y						1.0		100%
Jason Goon	y						1.0		100%
Jay Govani		y					1.0		100%
Lu Wang			y				1.0		100%
Yangyang Li					y	0.25		100%	
Michelle While*				y		0.5			
Kyler Kooi					y	0.25		100%	
Alex Kirkvold					y	0.25		100%	
Chaoyang Jiang	y						0.25	33%	
Rajendra Penth				y		0.5			

*: The funding sources are other than DOE and CUBED

5. An update list of other support

USD provided bridge funding to continue the project including CUBED funding that we reported to the DOE during the site visit review. In addition, the physics PhD funding has been used to support graduate students working on this project. This year, we have also participated in the NSF I-Corps program with an award of $50,000, which has supported a graduate student, a business mentor, and the PI for working on developing a business model for commercializing the grown crystals. Starting from October 2017, we have obtained a NSF PIRE grant of $4.35M.

6. Cost Status

USD received the official grant award in August of 2010. In eight years, we have spent 100% of the total budget. The table below shows the cost status for the entire project as of June 30, 2018 since 2010.

Items	Beginning Balance	Expenditures	Remaining Balance
Salaries	$1,208,891.46	-$1,208,891.46	$0
Benefits	$208,941.13	-$208,941.13	$0
Travel	$65,122.79	-$65,122.79	$0
Contractual	$39,011.43	-$39,011.43	$0
Grants and subsides	$137,491	-$137,491	$0
Supplies	$245,809.39	-$245,809.39	$0
Equipment	$711,740.72	-$711,740.72	$0
Tuition	$78,437.08	-$78,437.08	$0
Indirect	$728,933	-$728,0933	$0
Total	$3,424,378	-$3,424,378	$0

Given the above numbers in the table, our current cost status is 100% of the total budget for the entire grant period.